Seasonal Variability of Atmospheric Aerosol Parameters over Greater Noida Using Ground Sunphotometer Observations

Manish Sharma[1], Dimitris G. Kaskaoutis[2], Ramesh P. Singh[3*], Sachchidanand Singh[4]

[1] *Research and Technology Development Centre (RTDC), Sharda University, Greater Noida-NCR, 203201, India*
[2] *Department of Physics, School of Natural Sciences, Shiv Nadar University, Dadri-NCR, 203207, India*
[3] *School of Earth and Environmental Sciences, Schmid College of Science and Technology, Chapman University, One University Drive, Orange, CA 92866, USA*
[4] *Radio & Atmospheric Sciences Division, CSIR-National Physical Laboratory, New Delhi - 110012, India*

ABSTRACT

Atmospheric aerosols over northern India are subject of significant temporal and spatial variability and many studies have been carried out to investigate their physico-chemical and optical properties. The present work emphasizes on examining the aerosol optical properties and types over Greater Noida, Delhi region, using ground-based sun photometer data during the period 2010–2012. The analysis reveals a relatively high mean aerosol optical depth at 500 nm (AOD_{500} = 0.82 ± 0.39), associated with a moderate Angstrom exponent $\alpha_{440-870}$ of 0.95 ± 0.37. Both parameters, exhibit significant daily, monthly and seasonal variability with higher values of AOD_{500} during post-monsoon (0.98 ± 0.50) and winter (0.87 ± 0.35) seasons associated with high α values (> 1.1) suggesting significant urban and biomass-burning contribution. On monthly basis, the highest AOD is found during July and November and the lowest one in the transition months of March and September. The aerosol-type discrimination via the relationship AOD vs. α shows a clear dominance of urban/industrial and biomass-burning aerosols during post-monsoon and winter in fractions of 74.5% and 72%, respectively, while aerosols of desert-dust characteristics were most frequent in pre-monsoon (41.7%) and monsoon (21%) seasons. In general, the analysis shows a rather well-mixed aerosol type under very turbid atmosphere, which is associated with the long range transport of pollutants through the westerly winds from the Thar desert and biomass burning in the western parts of India.

Keyword: Atmospheric aerosols; Sunphotometer; Aerosol optical depth; Dust storm; AERONET; Dust; Biomass burning.

INTRODUCTION

Aerosols over India exhibit strong seasonal and inter-annual variability mainly driven by the regional monsoon system, atmospheric dynamics, seasonally-changed air-mass patterns and spatio-temporal distribution of emission sources (Ramachandran and Cherian, 2008; Kaskaoutis *et al.*, 2011). The Indo-Gangetic plain (IGP), in the northern part of India, is among the most densely populated as well as polluted and heavy aerosol-laden regions of the world (Gautam *et al.*, 2011). As a consequence, despite the deterioration in air quality and effects on human health and ecosystems, aerosols over the region may have serious climatic implications on the heating of the lower and mid troposphere, solar dimming, sea-land temperature gradients, cloud microphysics, monsoon circulation and distribution of rainfall (Lau *et al.*, 2006; Gautam *et al.*, 2010). Numerous studies examining the aerosol radiative forcing over India resulted in high spatio-temporal variability also exhibiting significant uncertainties, mainly due to the different sources, land use, aerosol types and properties as well as the influence of dynamic and synoptic meteorology and the mixing (internal and external) processes in the atmosphere (Lawrence and Lelieveld, 2010). With the increase in population, urbanization, industrialization and demands for energy, the aerosol loading over Indian sub-continent is gradually increasing, exhibiting large spatio-temporal variability in its trends (Kaskaoutis *et al.*, 2011; Ramachandran *et al.*, 2012; Moorthy *et al.*, 2013). In order to understand the dynamics and variability of aerosol, systematic measurements of aerosol properties are needed at many locations to support the validation of the satellite algorithms and the inputs in general circulation and chemical transport models.

The significant anthropogenic emissions, mainly from fossil fuel, bio-fuel burning and emissions from coal-based thermal power plants, composed of a significant amount of carbonaceous aerosols, sulfate and nitrate (Prasad *et al.*, 2007; Singh, 2010, Lu *et al.*, 2011; Prasad *et al.*, 2012) favor the existence of hazy conditions over the Ganges basin

---

* Corresponding author.
  E-mail address: Ramesh P. Singh rsingh@chapman.edu

during the most of the year, while the combination of low temperatures during winter lowering the relative humidity and dew point favor the frequent formation of dense fog (Gautam *et al.*, 2007). From April onwards the high-land temperatures over northwestern arid regions (Thar desert) favors the convection and uplift of dust aerosols, while in conjunction with intense surface winds, dust storms affect the region (Dey *et al.*, 2004; Prasad *et al.*, 2007; Prasad and Singh, 2007). The monsoonal rainfall usually starts by the mid of June over western IGP (Rajeevan *et al.*, 2006) and is able to partly decreasing of aerosol loading due to rain washout, despite the fact that during this season, the dust activity over Arabia and Middle East is at its maximum (Ginoux *et al.*, 2012), also affecting India. The main characteristic of the post-monsoon season is the agricultural burning of crop residue, especially in the state of Punjab, northwestern IGP (Kharol *et al.*, 2012), which affects the aerosol and chemical-pollution field over the region (Safai *et al.*, 2007). As a consequence, a variety of aerosol types is observed over IGP and some studies have attempted in their identification and classification over different locations (Giles *et al.*, 2011; Wang *et al.*, 2011; Srivastava *et al.*, 2012). On the other hand, the modification processes in the atmosphere, result in mixing of the coarse-mode natural particles with fine-mode anthropogenic aerosols (Dey and Tripathi, 2008; Srivastava and Ramachandran, 2012) in a well-mixed thick aerosol layer known as "Asian Brown Clouds" (ABC) (Ramanathan *et al.*, 2005). Therefore, considering the aerosol-type discrimination is a real challenge.

The mega-city Delhi, located in the northwestern part of IGP, has been recognized as one of the most polluted cities in India (Beegum *et al.*, 2009; Mishra *et al.*, 2013) with high levels of anthropogenic aerosols (Soni *et al.*, 2011; Srivastava *et al.*, 2012b), on which the dust entering in the region in pre-monsoon further deteriorates the air quality and enhances the radiative forcing (Singh *et al.*, 2005, 2010). The mostly-dominant western/northwestern winds transport the aerosols and pollutants over the southeastern Delhi suburban, which are highly developing areas, with huge construction activities. The increasing urbanization impacts Delhi surroundings and neighboring towns and villages, while the westerly winds bring pollutants to Greater Noida, which are mixed with the existing emissions coming from brick kilns and the nearby Dadri power plant. However, aerosol studies over this region, which is one of the emerging areas at the border of Delhi and Uttar Pradesh province, have not been published so far, except recent analyses over Gual Pahari AERONET (AErosol RObotic NETwork) station, located south of Delhi (Hyvärinen *et al.*, 2011a, b). In the present study, the seasonal variation of aerosol optical properties is examined for the first time over Greater Noida during the period 2010–2012. Daily spectral aerosol optical depth (AOD) data were measured using Microtops-II sun photometer and averaged to examine the monthly and seasonal variations as well as to discriminate different aerosol types.

STUDY REGION AND DATA RECORDING

The data were taken on the campus of Sharda University, Greater Noida (hereafter referred to as GN) (28.46°N, 77.48°E, 200 m amsl) located ~40 km southeast of New Delhi and ~15 km southwest of the Dadri power plant. The population of the region is ~293,908; the area is under the purview of Delhi, NCR (Fig. 1), with several small industries, mainly cement and brick factories, to contribute to significant aerosol and pollution emissions. This area is hub of educational centers with numerous Universities, Engineering colleges and research institutions. Despite the area is mostly rural-agricultural field, due to growing urbanization, industrialization, economic growth and rural-population migration, the aerosol and pollution levels over GN are high causing intense haze and foggy conditions, deteriorating the air quality and reducing the visibility especially during winter.

The winter (December–February) is chilly and very often cold waves from the Himalayan region drop the temperature as low as 3 to 4°C (mainly in January), which in combination
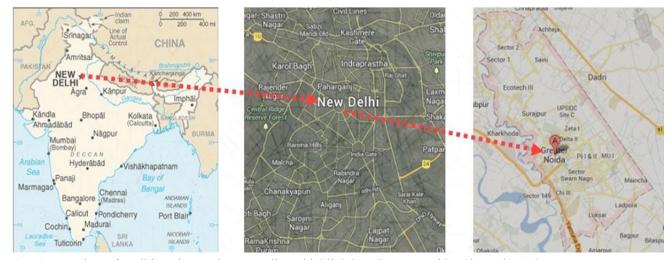

Fig. 1. Location of Delhi region and surroundings highlighting Greater Noida where the AOD measurements were performed.

with the low dew point, enhance the presence of dense fog being a daily phenomenon (http://www.greaternoidaweb.in/climate.aspx). During the winter months, burning of biomass, animal manure and wood is a common practice on the road side and houses, which increases the levels of black carbon concentration up to 20–25 µg/m³ (Singh and Sharma, 2012). During May and June, the temperature is very high, usually above 40°C, even reaching to 44–46°C on several days. Except of the suspended dust from the neighboring desert areas (Thar), strong surface winds cause local dust-storm events uplifting a huge amount of construction materials. Monsoon rainfall usually starts by the mid of June and lasts till end of September with an average of 800 mm (Rao *et al.*, 2011), while during post-monsoon the area is under the influence of agriculture burning. In general, the meteorology and climatic conditions in GN follow those of Delhi (Lodhi *et al.*, 2013).

Using Microtops-II (MT) sun photometer, spectral aerosol optical depth is measured during the period 2010–2012 on the campus of the Sharda University, GN. The sun photometer measures the direct solar irradiance at five wavelengths (440, 500, 675, 870 and 936 nm) using a narrow band of interference filters (Morys *et al.*, 2001). Complete details of the instrument and measurement techniques can be found in User Guide, MT-II sunphotometer version 5.5, Solar Light Company Inc. The filters have a peak wavelength precision of ± 1.5 nm and a full width at half maximum bandwidth of 10 nm. The spectral AOD is calculated via the instrument's internal calibration, while the theoretical and/or experimental errors in AOD are in the range of 0.002–0.021, with higher ones in the UV region (Morys *et al.*, 2001; Singh, *et al.*, 2010; Kaskaoutis *et al.*, 2011). The measurements were performed three times on daily basis (~9:00 in the morning, 13:00 at noon and 16:30 in the afternoon) under cloudless sky conditions and when the clouds were far from the sun disk. Some gaps in the data series exist, as during June 2010–March 2011, when the MT-II was out of order due to some technical problems and calibration procedure. After excluding some perturbed data (see next section), the remaining dataset consists of 818 spectral AOD scans, 165 during winter (Dec–Feb), 295 during pre-monsoon (Mar–May), 205 during monsoon (Jun–Sep) and 153 during post-monsoon (Oct–Nov).

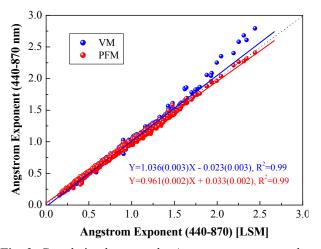## METHODOLOGY AND ERROR ANALYSIS

The MT sun photometer was used for the first time at Greater Noida and, therefore, efforts were made to take special care while making observations and also in the retrievals of spectral AODs and the computed parameters, i.e., Angstrom exponent, derivate of Angstrom exponent. In this section a discussion about the analysis and the accuracy of the retrievals takes place. In order to minimize errors from MT when it is targeting the sun, three to five scans were taken at each time. From these scans the one that exhibits a combination of lowest AOD and lowest error in the second-order polynomial fitting was selected as the least biased either from circumsolar radiation or from undetected thin cirrus clouds (cloud-contamination effect).

From the new dataset, the spectrums that calculate AODs and α beyond the daily mean +/– 2stdev (standard deviation) were also excluded from the analysis. During this stage the majority of the cases that were excluded correspond to high AODs (especially at longer wavelengths) and to very low α values suggesting cloud contamination. From the remaining cases, those that concluded to R2 values below 0.94 from the second-order polynomial fit to the lnAOD vs. lnλ were also excluded. Such cases are associated with low AOD and significant curvature in the lnAOD vs. lnλ curve, Eq. (2) (Schuster *et al.*, 2006; Kaskaoutis *et al.*, 2010, 2011).

Since spectral AOD presents a curvature in log-log coordinates due to inaccuracies in the fit of the Angstrom's formula, Eq. (1) (Kaskaoutis and Kambezidis, 2006) the consistency in the retrievals of Angstrom exponent via different methods gives credit to the accuracy of the spectral AOD retrievals and minimizes the curvature effect (Kaskaoutis and Kambezidis, 2008). Here, we correlate the α values obtained via the least-squares method (LSM, total use of four wavelengths) with those obtained via the Volz method (VM, use of two wavelengths) and those obtained via the polynomial fit method (PFM, $a_2 - a_1 = α$ (according to Schuster *et al.*, 2006) (Fig. 2).

$$AOD_λ = βλ^{-α} \text{ or } lnAOD = -αlnλ + lnβ \tag{1}$$

$$lnAOD_λ = a_2(lnλ)^2 + a_1lnλ + a_o \tag{2}$$

The results show an excellent agreement ($R^2 = 0.99$) between the computed parameters with RMSD (Root Mean Square Difference) of 0.015 and 0.025 for the correlation between the LSM and VM and between LSM and PFM, respectively. The slope values close to 1 and the negligible intercept indicate great accuracy in the retrievals of α and, therefore, to the spectral AOD. Only a few cases determined

Fig. 2. Correlation between the Angstrom exponent values obtained via different techniques in the wavelength range 440–870 nm. The data cover the whole period of measurements (2010–2012), total number of 931 spectral recordings, before excluding the perturbed data. [LSM: Least-squares method; VM: Volz method; PFM: polynomial fit ($a_2 - a_1$) method].
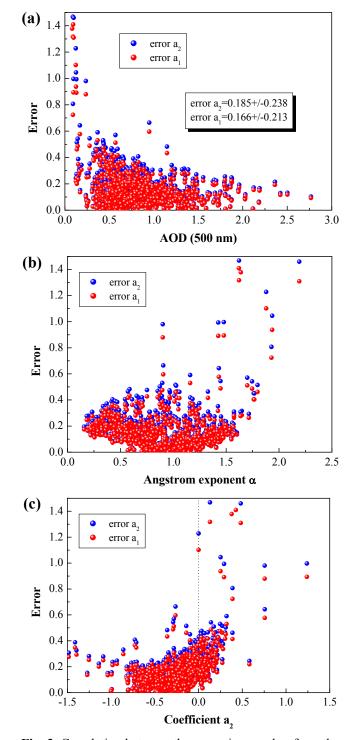
via VM seem to depart from the linearity, while the maximum error in α retrievals is ~0.12. The relationship $a_2 - a_1 = \alpha$ has been used for checking the validity of the retrievals (Schuster *et al.*, 2006; Kaskaoutis *et al.*, 2011), while the consistency in α between the LSM and VM suggests negligible curvature effect and low spectral variation of α (Kaskaoutis and Kambezidis, 2008).

Figs. 3(a)–3(c) show correlation between errors in a_1 and a_2 retrievals (Eq. (2)) with AOD_{500}, Angstrom exponent, and curvature, respectively, examining the atmospheric conditions resulting in higher inaccuracies in the aerosol retrievals. Both errors vary in the range 0.002 to 0.6, with that for a_2 to be slightly higher. For very few cases in September 2011, the error is above 0.6 associated with low (< 0.2) AOD_{500} values. In general, there is a tendency for decreasing error and better simulation of Eq. (2) under more turbid conditions (Kaskaoutis *et al.*, 2010), while there is no such a tendency as a function of α; however, nearly the whole cases with large errors correspond to high (> 1.5) values of α. Similar feature is revealed from the correlation between errors and coefficient a_2, where the error seems to be higher for increasing negative curvature and for high positive values of a_2. Overall, the results show that the dataset is robust enough and the errors are negligible for the purposes of the current work.

RESULTS AND DISCUSSION

Severe Aerosol Loading over Greater Noida

The daily-mean variations of AOD_{500} and $\alpha_{440-870}$ (Fig. 4) during Jan 2010 to Dec 2012 over Greater Noida show a large scatter in both parameters due to large variability in atmospheric conditions, emission rates, boundary-layer dynamics and long-range transport. As far as AOD_{500} is concerned the values range from as low as ~0.08 to as high as ~2.77, revealing a mean of 0.82 ± 0.39. The very low AOD values were found only on few days, while 574 out of the 818 AOD_{500} data (70%) are above 0.6 indicating a severe aerosol-laden atmosphere over Greater Noida, despite the mostly rural environment of the region. Similar range of values and fraction of $AOD_{500} > 0.6$ are reported for urban Delhi (Lodhi *et al.*, 2013) suggesting that Delhi pollution strongly influences atmospheric aerosol of Greater Noida. The construction activities throughout the region as well as the proximity (~15 km) with the Dadri power plant may also contribute to the high AODs over Greater Noida, while the influence of the local traffic and vehicular emissions is expected to be much lower than that over other urban Indian environments. The mean AOD is higher than those reported over Kanpur (Singh *et al.*, 2004; Eck *et al.*, 2010; Giles *et al.*, 2011; Kaskaoutis *et al.*, 2012) and Gandhi College (Srivastava *et al.*, 2011, 2012), which are considered as highly polluted regions in IGP as well as than those reported over several Indian cities (Moorthy *et al.*, 2013). Values of AOD at the level of ~0.8 were reported for Delhi (Singh *et al.*, 2005, 2010) and during specific events of dust storms (Dey *et al.*, 2004; Prasad and Singh, 2007; Badarinath *et al.*, 2010, Sharma *et al.*, 2012) and/or biomass burning (Kharol *et al.*, 2012) over IGP region. Even the 30-

days moving average shows significant peaks and gaps on specific months, highlighting high aerosol episodes in June–July of 2011 and Oct–Nov of 2011 and, especially, 2012.

Fig. 3. Correlation between the errors in a_2 and a_1 from the second-order polynomial fit to lnAOD vs. lnλ with the AOD_{500} (a), Angstrom exponent (b) and coefficient a_2 (c). Cases prone to cloud contamination or to not accurate targeting of the sun, resulting to inaccuracy in the fitting have been excluded from the analysis.
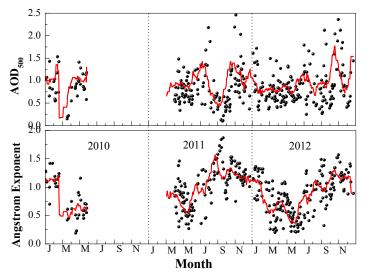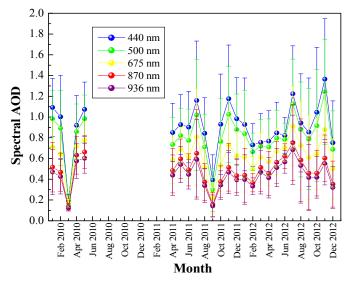
Fig. 4. Time series of the daily-averaged AOD_{500} and $\alpha_{440-870}$ over Greater Noida during 2010–2012. The red line corresponds to 30-days moving average.
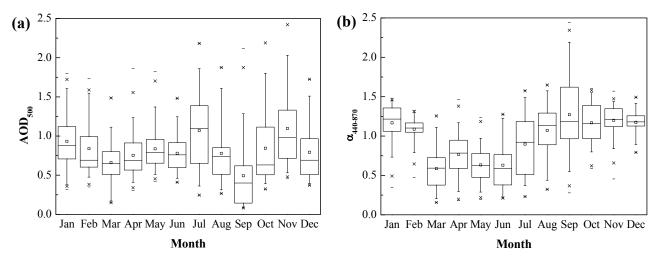
The Angstrom exponent α shows a more distinct seasonal variability with values ranging from ~0.15 to ~1.5, while in few days the mean value is beyond this upper limit. The large variability indicates significantly seasonal or even daily-changed atmospheric conditions and dominance of aerosol of different size, composition and optical properties. High values of α are observed during post-monsoon and winter seasons accompanied with low values during late pre-monsoon and monsoon seasons due to influence of dust, following the usual scenario over IGP (Soni *et al.*, 2011; Kaskaoutis *et al.*, 2012; Lodhi *et al.*, 2013). The mean value of $\alpha_{440-870}$ was found to be 0.95 ± 0.37, comparable to the yearly mean values that observed over other sites in IGP, like Delhi (Singh *et al.*, 2010), Kanpur (Singh *et al.*, 2004; Kaskaoutis *et al.*, 2012), and far East to Dibrugarh (Gogoi *et al.*, 2009). Considering the whole set of observations, it is characteristic that α is nearly equally distributed around 1.0, with the 52% of the values to be below 1.0.

The remarkable daily variability in AOD_{500} and $\alpha_{440-870}$ values as shown in Fig. 4 is impressed in the monthly-mean spectral AOD variation for all five available MT wavelengths (Fig. 5). The seasonal-changed dominance of fine or coarse aerosols has a direct effect on the temporal variability in AODs at shorter and longer wavelengths as well as in the gradient between them, since seems to be larger during post-monsoon and winter months. In contrast, lower gradient corresponding to more neutral AOD spectra is found during April to August months. A significant gap in spectral AOD data series is found in March 2010 and September 2011, when relative clean conditions dominated over Greater Noida. Due to larger variations in light scattering caused by changes in fine-mode aerosols (Schuster *et al.*, 2006), the monthly variability of AOD_{440} is more intense than that at 936 nm, ranging from as low as ~0.3 (March 2010) to as high as ~1.4 (November 2012). More or less similar pattern of the spectral AOD variation has been found over Delhi (Lodhi *et al.*, 2013), Hyderabad (Sinha *et al.*, 2012), Ahmedabad (Ganguly *et al.*, 2006), Dibrugarh

(Gogoi *et al.*, 2009), Kullu valley (Guleria *et al.*, 2011), Varanasi (Tiwari and Singh, 2013), Pune (Dani *et al.*, 2012), Bangalore (Vinoj *et al.*, 2004), among many others.

The AOD_{500} and $\alpha_{440-870}$ values are summarized on monthly basis and plotted in box and whisker charts (Figs. 6(a) and 6(b)), providing concurrent information about the mean, median and the range of the values. Very high monthly-mean AOD_{500} values, ranging from ~0.5 (September) to ~1.1 (July, November) are found over Greater Noida during the period 2010-2012. The annual AOD pattern seems to be tri-modal with maximum values in July, November and January and lowest ones in the transition months of March and September. This annual pattern is characteristic for the IGP sites as long-term climatology studies covering about a decade over Delhi (Lodhi *et al.*, 2013) and Kanpur (Giles *et al.*, 2011; Wang *et al.*, 2011). This pattern indicates the significant influence of dust during late-pre-monsoon and in the beginning of the monsoon. The feature that differentiates IGP from other regions (rural and urban) in the rest of India is the very high late post-monsoon and winter AODs, also clearly detected by satellite remote sensing (Goloub *et al.*, 2001; Kaskaoutis *et al.*, 2011), mainly consists of fine-mode anthropogenic aerosols from fossil fuel and bio-fuel burning (Dey and Tripathi, 2008). There is a tendency of decreasing AOD during the transition season of winter to pre-monsoon, since during that period (March and beginning of April) the extensive burning of bio-fuels for heating purposes has terminated and the dust activity has not yet started. Similarly, by the end of August and during September, the dust activity in Arabia and Thar is progressively reducing and the monsoon rain has acted as ventilation tool for the aerosol washout. As a consequence, the transparent atmospheric conditions are more frequent before the agriculture crop residue burning starts by the beginning of October (Sharma *et al.*, 2010; Kharol *et al.*, 2012). However, the current analysis is based on 25-months of AOD observations and may differentiate considering a much longer period, despite the large consistency that it

Fig. 5. Monthly variation of the spectral AOD values over Greater Noida during the period 2010–2012. The vertical bars exhibit one std from the monthly mean.

Fig. 6. Box and whisker graph of the monthly AOD_{500} (a) and the Angstrom exponent (b) values over Greater Noida during the period 2010–2012.
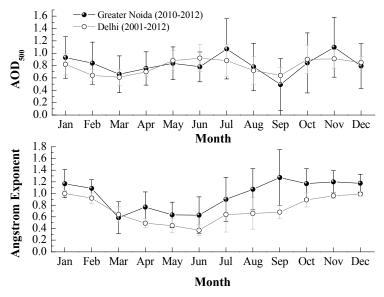
shows with the annual pattern found over Delhi (Lodhi *et al.*, 2013). Furthermore, some extreme values of AOD (> 2.0) may influence the monthly means in July and November, which are the months with the highest variation in AOD. The mean AOD in October and November is significantly above the median values, indicating a shift towards larger values attributed to the massive smoke plumes over IGP during the burning period of Oct–Nov 2012 whereas much lower AOD is observed during Jan–May period.

The annual-mean pattern for the Angstrom exponent (Fig. 6(b)) highlights the large (> 1.0) post-monsoon and winter values and the low (< 0.7) pre-monsoon and early monsoon ones. Although such annual variability is common over IGP, some differences from location to location are observed due to the long-range dust transport, the local anthropogenic emissions and the dynamics of the boundary layer (Kaskaoutis *et al.*, 2009), indicating the dominance of fine-mode aerosols during post-monsoon and winter and

the coarse particles during the rest of the year. The range in α values is much higher during monsoon months indicating large variability in the source regions, aerosol types and optical characteristics, while more homogeneous atmosphere, with very low variation in α is found during late post-monsoon and winter. Similar conditions about homogeneity in the sources and aerosol properties during the cold period of the year were observed over Kanpur (Kaskaoutis *et al.*, 2012), Hyderabad (Sinha *et al.*, 2012), Dibrugarh (Pathak *et al.*, 2013) and, in general, over the whole India as found via satellite observations. The largest monthly mean $\alpha_{440-870}$ value is shown in September (1.27 ± 0.47) attributed to some extreme values (above 2.0) during September 2011. This is the main difference from the annual pattern found over Delhi (Lodhi *et al.*, 2013) during the period 2001–2012. In general, the current α values are 0.1–0.4 higher, on monthly basis, than those observed over Delhi, with these differences to be much higher than the respective ones in AOD_{500} (Fig. 7).

This indicates the most sensitivity of α on changes in atmospheric composition, scattering processes as well as in the wavelength region used for its determination, which is at 340–1020 nm in Lodhi *et al.* (2013). The AOD_{500} monthly-mean values show a great consistency between Delhi and Greater Noida, while limiting the comparison in the common months the two datasets exhibit a high correlation ($r = 0.74$). However, it should be noted that the two datasets cover different time periods, while some "extreme" values on specific months can influence the monthly mean, especially for the shorter time dataset over Greater Noida.

The seasonal-mean spectral AOD distribution is shown in Fig. 8. Such a pattern was expected from the previous analysis of the AOD and α values for each month, indicating higher values at shorter wavelengths (440 nm) for post-monsoon and winter compared to pre-monsoon and monsoon. Such evidence is rather characteristic for the IGP sites, as

shown in Kanpur (Wang *et al.*, 2011) and Varanasi (Tiwari and Singh, 2013), but opposite to that found over central-south India (Sinha *et al.*, 2012), where the pre-monsoon spectral AOD dominates. In the current analysis, it is shown that the post-monsoon AOD is highest even at 675 nm, highlighting the significant influence of the intense smoke plumes covering nearly the whole IGP in November 2012. On the other hand, at longer wavelengths (870 nm), the seasonal mean AODs are similar (~0.5), suggesting that the larger gradient in spectral AOD during post-monsoon and winter is attributed mainly to the large increase in AOD at shorter wavelengths. The AOD_{500} is highest in post-monsoon (0.98 ± 0.50), associated with the highest seasonal α (1.18 ± 0.22), followed by winter (0.87 ± 0.34) and pre-monsoon (0.78 ± 0.28). However, in all seasons the standard deviations are very large considering their between differences in mean AODs rather meaningful. This

Fig. 7. Monthly mean variation of the AOD_{500} and α values obtained over Greater Noida during Jan 2010–Dec 2012 (present study) and Delhi during Dec 2001–May 2012 (Lodhi *et al.*, 2013). The vertical bars express one standard deviation from the monthly mean.
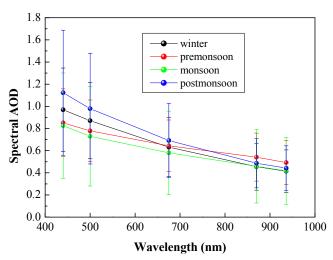

Fig. 8. Seasonal mean spectral AOD distribution over Greater Noida during the period Jan 2010–Dec 2012.

necessitates systematic aerosol observations over Greater Noida for a long time, in order to smooth the fluctuations caused by specific atmospheric phenomena (smoke and/or dust plumes) in certain periods. For comparison of observed aerosol optical depth and angstrom exponent (α) at Greater Noida with other locations in the Indo-Gangetic plains and in the surrounding regions, Table 1 is compiled based on the publish results. This table gives AOD and angstrom exponent for different seasons. The present results clearly show higher aerosol optical depth compared to cities located in the south of India and central parts of India, The aerosol optical depth is also higher compared to cities in the eastern parts of the Indo-Gangetic plains. The aerosol parameters also show influence of dusts which are more prevalent during the pre-monsoon season after comparing with other locations in the eastern parts of the Indo-Gangetic plains.

Dominant Aerosol Types

Aerosols originated from different sources exhibit highly different optical and physico-chemical properties, also being wavelength dependent (Dubovik *et al.*, 2002). The correlation between two intensive or extensive aerosol properties makes their characterization easier, although in the majority of the cases a well-mixed aerosol type, which is rather difficult to be classified occurs (Holben *et al.*, 2001). The most common scatter plot for the aerosol type discrimination is that between AOD and α (Kaskaoutis *et al.*, 2007a), while other techniques have also been used, like the wavelength dependence of single scattering albedo, SSA, the correlation between Fine-mode fraction and SSA (Lee *et al.*, 2010) and the correlation between absorption and extinction Angstrom exponent (Giles *et al.*, 2011). In all these techniques, some threshold values are considered for the discrimination between the aerosol types, which may differ depending on location, aerosol characteristics and range of AOD (Kaskaoutis *et al.*, 2009). In the present study, the scatter plot between AOD_{500} and $α_{440-870}$ was used for aerosol discrimination over Greater Noida. For the aerosol-type characterization, the same thresholds as in Kaskaoutis *et al.* (2009) over Hyderabad have been used, mainly because of the similarity between the two environments in the AOD and α levels. Thus, cases with AOD < 0.3 and α < 0.9 are considered to represent background conditions (BC), while AOD > 0.5 associated with α > 1.0 correspond to urban industrial and/or biomass burning aerosols (UI/BB). The detection of desert dust (DD) is associated with AOD > 0.6 and α < 0.7, while the cases not belonging in any of the above groups are considered as mixed type or undetermined (MT/U) aerosols.
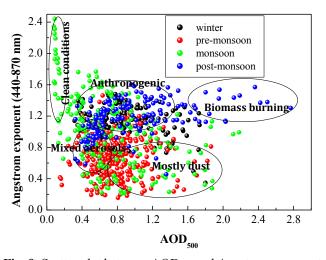
The AOD_{500} vs. $α_{440-870}$ scatter plot (Fig. 9) reveals a different pattern of scattering points depending on season. In some parts of the scatter plot, the atmospheric conditions and aerosol type are rather easily determined, as the clean conditions associated with AOD_{500} < 0.2, some cases associated with high AOD and α characteristic of biomass plumes contamination and cases with high AOD and low α dominated by desert or suspended dust. Cases mostly dominated by anthropogenic aerosols can also be discriminated, while a high-density area for intermediate

AOD and α values corresponds mostly to mixed aerosols via several processes in the atmosphere, that flatten out their original characteristics. The current scatter plot is not shifted towards a clear aerosol-type dominance, but rather constitutes a synthesis of the AOD vs. α scatter plots found over marine, urban, desert and biomass-burning environments (Kaskaoutis *et al.*, 2007a). As a consequence, the values of α exhibit a wide range (~0.3–1.6) for about the whole AOD range, while their between correlation (i.e., AOD vs. α) was found to be neutral. This suggests various sources of aerosols, which seem to be seasonally dependent as the analysis of air mass trajectories and potential hot-spot regions over Delhi shown (Lodhi *et al.*, 2013). More specifically, the Concentration Weighted Trajectory (CWT) analysis has shown that the hot-spot regions for high AOD over Delhi are mostly local and/or regional, consisted of areas located in northwest IGP and Pakistan, suffering from anthropogenic pollution (Gautam *et al.*, 2007) and seasonal biomass burning, mostly in post-monsoon (Sharma *et al.*, 2010). During the pre-monsoon and monsoon seasons, the Thar desert and Arabian Peninsula have a significant contribution in enhancing the AOD in Delhi region, since even the marine air masses are significantly dust-aerosol laden (Tiwari *et al.*, 2009).
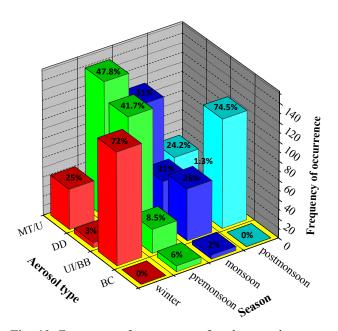
The seasonally-changed air masses and the potential contribution of various sources in the aerosol field over IGP have as a consequence the dominance of aerosols of different type and characteristics, which alters proportionally to season (Fig. 10). The analysis reveals that the UI/BB clearly dominates in post-monsoon (74.5%) and winter (72%) and in some fraction (26%) during monsoon seasons, while the DD type exhibits its highest presence during pre-monsoon (41.7%) and more rarely (21%) during monsoon and is nearly absent during the rest of the year. It is very interesting to note that clean background conditions are absent during post-monsoon and winter; a few cases of clean transparent atmospheres are found during pre-monsoon (mainly in March) and monsoon (in September). The majority of the cases not belonging to any of the above aerosol types (MT/U) is found during pre-monsoon and monsoon (~48-51%), while in the rest of the year this fraction is about 25%. However, it should be noted that the current fractions may be considered rather qualitatively and not quantitatively, since they correspond to specific threshold values, while an alteration in the thresholds would have cause changes in the fractions, but not in the general pattern of the seasonal distribution of aerosol types. A comparison of the present results with similar analysis performed over other locations in India is not an easy task due to different land use and environmental characteristics, differences in the time periods of the observations and in the seasonal pattern of the air masses and long-range transport, the specific influence of anthropogenic, industrial, biomass burning and dust over the different environments, the onset, duration and intensity of the monsoon over the country, etc. Note also, that the several studies may have used different techniques, thresholds and aerosol types. Nevertheless, a qualitative comparison and discussion between our results and those from other studies is attempted in the following.

Table 1. Shows aerosol optical depth (AOD) at 500 nm and angstrom exponent (α) for different places in Indo-Gangetic places and its surroundings reported by different authors.

Location	Period	Winter (AOD)	Pre-monsoon (AOD)	Monsoon (AOD)	Post-monsoon (AOD)	Winter (α)	Pre-monsoon (α)	Monsoon (α)	Post-monsoon (α)	Reference
Ahmedabad	2002–2005	0.32	0.42	0.43	0.43	1	0.3	0.4	1	Ganguly *et al.* (2006)
Kanpur	2001–2003	0.57	0.54	0.66	0.63	1.26	0.6	0.66	1.12	Singh *et al.* (2004)
Dibrugarh	2001–2007	0.31	0.45	0.25	0.19	1.14	0.85	0.87	1.12	Gogoi *et al.* (2009)
Delhi	2001–2012	0.77	0.78	0.74	0.91	0.97	0.49	0.66	0.93	Lodhi *et al.* (2013)
Hyderabad	2008–2009	0.48	0.57	0.51	0.5	1.04	0.9	0.84	1.01	Sinha *et al.* (2013)
Hyderabad	2009–2010	0.39	0.53	0.37	0.37	1.41	1.11	0.67	1.26	Sinha *et al.* (2012)
Kullu Valley	2006–2009	0.2	0.34	0.26	0.21	1.13	0.9	1	1.42	Guleria *et al.* (2012)
Kanpur	2009		0.50–0.69				0.45–0.74			Srivastava *et al.* (2011)
Gandhi College	2009		0.51–0.77				0.65–0.91			Srivastava *et al.* (2011)
Kanpur	2001–2005	0.61	0.57	0.65	0.67	1.25	0.57	0.7	1.25	Kaskaoutis *et al.* (2012)
Kanpur	2006–2010	0.63	0.59	0.6	0.76	1.24	0.66	0.77	1.27	Kaskaoutis *et al.* (2012)
Patiala	Oct 2006				0.76				1.1	Sharma *et al.* (2010)
Patiala	Oct 2007				0.97				1.31	Sharma *et al.* (2010)
Patiala	2008				0.81					Sharma *et al.* (2012)
Patiala	2009				0.64					Sharma *et al.* (2012)
Jaipur	2009		0.46				0.31			Gautam *et al.* (2011)
Chitkara	2009		0.57				0.72			Gautam *et al.* (2011)
Gual Pahari	2009		0.64				0.52			Gautam *et al.* (2011)
Kanpur	2009		0.61				0.57			Gautam *et al.*(2011)
Gandhi College			0.6				0.77			Gautam *et al.* (2011)
Greater Noida	**2010–2012**	**0.87**	**0.78**	**0.73**	**0.98**	**1.13**	**0.68**	**1.02**	**1.19**	**Present study**

Fig. 9. Scatter plot between AOD$_{550}$ and Angstrom exponent at 440–870 nm for the discrimination of different aerosol types over Greater Noida.

Fig. 10. Frequency of occurrence of each aerosol type on seasonal basis over Greater Noida during the period January 2010–December 2012.

Previous studies have used a density contour plot representation of the AOD vs. α over Indian sub-continent for identifying density-maximum areas corresponding to different aerosol types (Kaskaoutis *et al*, 2009, 2011); Vijaykumar and Devara, 2013). Kaskaoutis *et al.* (2009) have used the same thresholds for aerosol-type identification over urban Hyderabad; thus, a direct comparison of aerosol types between Greater Noida and Hyderabad is easier. The aerosols over Hyderabad were mostly in the mixed type in all seasons, with dominance during post-monsoon (72.9%) and winter (62.2%), while the highest frequency of UI/BB (47.2%) was detected during pre-monsoon and the DD (30.3%) during monsoon. Furthermore, the maritime-influenced aerosols and the transparent atmospheric

conditions were more common over Hyderabad compared to Greater Noida, due to larger influence by the southwest summer monsoon. The main differences in the seasonal variation of the UI/BB and DD aerosol types between Greater Noida and Hyderabad are attributed to the much lesser influence of Hyderabad (located in central-south India) by the dusty air masses originated from Thar and Arabia (Badarinath *et al.*, 2010) and, to the rather weak influence of Punjab smoke plumes during post-monsoon. Nevertheless, Hyderabad is mostly affected by the forest fires in Orissa during the dry pre-monsoon season (Kharol, *et al.*, 2012) at the time that Greater Noida is under the influence of frequent dust storms.

Mishra and Shibata (2012) have classified three aerosol types (dust, biomass burning and urban pollution) over Kanpur by analyzing the spectral variation of the absorbing Angstrom exponent (AAE) and extinction Angstrom exponent (EAE) values along with columnar size distribution based on 5-year (2006–2010) AERONET data. They found enhanced presence of dust aerosols during the pre-monsoon and monsoon seasons, dominance of urban/industrial pollution during winter season and enhanced biomass burning along with urban pollution during post-monsoon, thus indicating large similarities with the present analysis. Similarly, Giles *et al.* (2011) grouped the aerosols over Kanpur in three categories in the framework of TIGERZ experiment, viz. i) mostly dust, ii) mixed black carbon and dust and, iii) mostly black carbon using AAE, EAE, fine-mode fraction and sphericity fraction, showing that the dust contaminated aerosols have a clear pre-monsoon (April–June) dominance, while the black carbon aerosols were most abundant during the rest of the year. Aerosols of mostly anthropogenic origin were found at a high-altitude location over Pune during the period November 2009–April 2010 (Vijaykumar and Devera, 2013), while the seasonal variability of aerosol types over Dibrugarh (Pathak *et al.*, 2012) revealed dominance of UI aerosols during winter and pre-monsoon and dominance of MT during the rest of the year. It should be noted that Pathak *et al.* (2012) discriminated 5 aerosol types (continental average, marine continental average, urban/industrial-biomass burning, desert dust, and mixed type) and the differences compared to our results are mainly attributed to the different environments, climatology conditions, land use and long-range transport between northwest and northeast India. Via Optical Properties of Aerosol and Clouds (OPAC) simulations, Ramachandran *et al.* (2012) reported high contribution of the black carbon (36–37%) and mostly-anthropogenic water soluble (45%) aerosols to the total AOD during post-monsoon and winter over Ahmedabad, an urban location in western India. Similar to our observations, the contribution of dust to total AOD and aerosol mass was much more intense (36% and 76%, respectively) during the pre-monsoon season. Srivastava *et al.* (2012) discriminated four (polluted dust, polluted continental, mostly black carbon and mostly organic carbon) aerosol types over Kanpur and Gandhi College AERONET sites, but only for the pre-monsoon season, by the combination of relationships between fine-mode fraction and SSA and AOD and α, revealing as the most dominant aerosol type
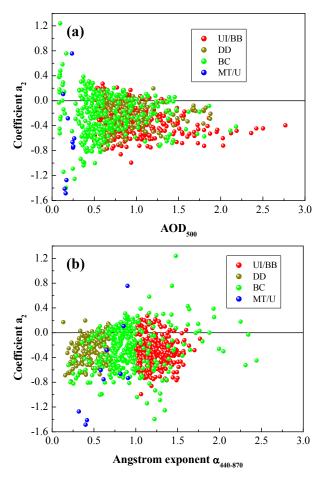
the polluted dust (62%) over Kanpur and the polluted continental (46%) over Gandhi College.

Table 2 summarizes the main aerosol properties for each aerosol type and season. The AOD_{500} seems to be very high during some few DD events in post-monsoon and winter, usually associated with strong surface winds also carrying mineral dust from the several constructions around Greater Noida. On the other hand, the lowest AOD from the MT/U aerosol type during monsoon indicates that these conditions are associated with moderate turbid atmospheres, in contrast to that found during post-monsoon, when a mixture of aerosols takes place under a turbid environment. Note also the much higher AOD value for the UI/BB aerosol type in post-monsoon compared to the other seasons, which is influenced by the dense smoke plumes over western IGP during post-monsoon of 2012. The values of α do not differ significantly between the seasons for the same aerosol types, while those determined at longer wavelengths (675–870) give a more clear view of the fine-to-coarse mode ratio against those at shorter wavelengths that are much more sensitive in changes in aerosol fine-mode radius (Schuster *et al.*, 2006). An interesting finding is the negative mean a_2 values for each aerosol type and season, suggesting a large contribution of fine-mode particles in the lnAOD wavelength dependence.

Eck *et al.* (2001) have shown the importance of using the coefficient a_2 (obtained from Eq. (2)) along with AOD and α for the better aerosol discrimination, especially for intermediate values of α. Therefore, a similar approach is attempted on the spectral AOD data series over Greater Noida. Fig. 11(a) shows the scatter plot between AOD and coefficient a2 for the four aerosol types, while Fig. 11(b), the respective graph as a function of α. A hodgepodge of AOD

and a_2 values is shown in Fig. 11(a), except of some few cases which can be easily discriminated (UI/BB aerosols). The range and pattern distribution of a_2 values does not allow a further discrimination of the aerosol types, since similar range of a_2 is shown for all aerosol types for values of AOD between 0.4 and 1.5. However, the large range of a_2 values in the lower AODs tends to decrease and be constant at about –0.5 for AOD > 2.0. Same results are revealed from the scatter plot between α and a_2, since the different types are much easier discriminated depending on α rather than a_2. Thus, the use of the curvature as an additional tool for the aerosol-type discrimination over Greater Noida is not so applicable, suggesting aerosols of well-mixed type in the majority of the cases. A main finding on this aspect is that even the aerosols of desert dust properties exhibit negative a_2 values suggesting concave-type curve in the lnAOD vs. lnλ with curvature similar to that for urban and biomass-burning aerosols. This indicates significant external and/or internal mixture of dust with anthropogenic aerosols over the region. Such mixing is very likely due to dust and anthropogenic emissions from Delhi and surroundings of the measurement site, especially from Dadri power plant and brick kilns. In contrast, curvature was proved as useful for the identification of aerosols over Hyderabad (Kaskaoutis *et al.*, 2009), Arabian Sea (Kaskaoutis *et al.*, 2010) and Bay of Bengal (Kaskaoutis *et al.*, 2011), as well as for regions with very differing aerosol types (Kaskaoutis *et al.*, 2007b). A better understanding of the aerosol optical, physical and chemical properties and their linkage to meteorological dynamics needs further analysis from ground-based instruments, satellite observations and model simulations as well as examination of the role of meteorology in such interactions.

Table 2. Aerosol optical properties of the different aerosol types on seasonal-mean basis over Greater Noida during the period January 2010–December 2012.

Type	AOD	α (440–870)	Coefficient a_2	α (440–675)	α (675–870)
Winter					
BC					
UI/BB	0.902 ± 0.289	1.206 ± 0.124	–0.398 ± 0.135	1.087 ± 0.109	1.399 ± 0.177
DD	1.071 ± 0.606	0.526 ± 0.134	–0.309 ± 0.171	0.492 ± 0.112	0.579 ± 0.217
MT/U	0.759 ± 0.424	1.010 ± 0.184	–0.473 ± 0.203	0.884 ± 0.164	1.213 ± 0.262
Pre-monsoon					
BC	0.206 ± 0.051	0.525 ± 0.182	–1.032 ± 0.401	0.259 ± 0.282	0.912 ± 0.106
UI/BB	0.821 ± 0.216	1.145 ± 0.109	–0.107 ± 0.209	1.124 ± 0.126	1.190 ± 0.155
DD	0.874 ± 0.214	0.489 ± 0.144	–0.229 ± 0.218	0.485 ± 0.166	0.509 ± 0.165
MT/U	0.712 ± 0.278	0.760 ± 0.187	–0.263 ± 0.286	0.722 ± 0.229	0.843 ± 0.191
Monsoon					
BC	0.201 ± 0.054	0.829 ± 0.119	–0.038 ± 0.631	0.860 ± 0.250	0.913 ± 0.229
UI/BB	0.855 ± 0.289	1.267 ± 0.196	–0.282 ± 0.289	1.181 ± 0.189	1.459 ± 0.298
DD	1.058 ± 0.308	0.427 ± 0.127	–0.297 ± 0.193	0.406 ± 0.142	0.483 ± 0.141
MT/U	0.549 ± 0.446	1.135 ± 0.469	–0.167 ± 0.424	1.098 ± 0.471	1.339 ± 0.702
Post-monsoon					
BC					
UI/BB	1.115 ± 0.491	1.272 ± 0.149	–0.311 ± 0.249	1.175 ± 0.169	1.448 ± 0.187
DD	1.297 ± 0.144	0.557 ± 0.144	–0.045 ± 0.025	0.606 ± 0.123	0.488 ± 0.173
MT/U	1.115 ± 0.188	0.952 ± 0.189	–0.144 ± 0.265	1.936 ± 0.225	1.019 ± 0.201

Fig. 11. Correlation of the coefficient a_2 with AOD_{500} (a) and Angstrom exponent (b) for different aerosol types.

a concave type curve in the lnAOD vs. lnλ. The nearby to the study region Dadri power plant (this power plant has six units, use coal as well as gas with 830 MWe) and several small industries and brick factories control the aerosol field and properties as well as the intensive construction activities (building of new cities) around the study site. Being also in the downwind region of the pollution outflow from the Delhi megacity, the high aerosol loading, which is comparable to that found over Delhi, can be justified. Special care was taken in excluding any perturbed irradiance data by comparing the retrievals of α via several methods and eliminating the errors in the second-order polynomial fit of the spectral AOD in a log-log plot. The remaining dataset after excluding the perturbed data, consisted of 818 daily observations, was further used for the discrimination and classification of the main aerosol types (urban/industrial-biomass burning, desert dust and background) by means of the AOD vs. α scatter plot on seasonal basis. The analysis revealed dominance of urban-biomass aerosols during post-monsoon and winter (> 70%), while the dust aerosol type was more frequently occurred during pre-monsoon (42%). However, in the majority of the cases aerosols were not easily to be discriminated in any of the above types and rather well-mixing atmospheric conditions dominated. The present results are in reasonable agreement with those reported for sites in the Ganges basin, but they exhibit considerable variations with aerosol composition and types over other environments in India. Nevertheless, the current analysis highlights the specific role that the population density, industries, power plants and urban environments play in the high aerosol loading even over rural environments in the Ganges basin.

CONCLUSIONS

The present study examined the seasonal variation of the aerosol optical properties as well as the aerosol types over Greater Noida, Delhi-NCR, India. Systematic daily measurements of spectral AOD were performed at the study site, located in the Sharda University campus, covering the period January 2010 to December 2012, with some gaps in data. The results revealed a significant daily, monthly and seasonal variability of the aerosol loading and Angstrom wavelength exponent, with higher values of AOD and α during post-monsoon (0.98 ± 0.5) and winter (0.87 ± 0.34), while the mean AOD_{500} value of 0.82 ± 0.39 indicates a very turbid environment influenced by aerosols of different size, composition and source region (mean value of $\alpha_{440-870}$ = 0.95 ± 0.37). More specifically, during post-monsoon and winter the fine-mode aerosols clearly dominated, mainly originated from anthropogenic emissions (fossil fuel and bio-fuel combustion) and/or intense agriculture biomass burning as was the case in November 2012. During pre-monsoon and monsoon seasons, dust (either locally produced or long-range transported) has a significant contribution to the total AOD, thus reducing the α values (0.67 ± 0.25, in pre-monsoon). However, in the vast majority of the cases (~82%) the aerosols were mostly of fine-mode considering

REFERENCES

Badarinath, K.V.S., Kharol, S.K., Kaskaoutis, D.G., Sharma, A.R., Ramaswamy, V. and Kambezidis, H.D. (2010). Long-range Transport of Dust Aerosols over Arabian Sea and Indian Region - A Case Study Using Satellite Data and Ground-based Measurements. *Global Planet. Change* 72: 164–181.

Beegum, S.N., Moorthy, K.K., Babu, S.S., Satheesh, S.K., Vinoj, V., Badarinath, K.V.S. *et al.* (2009). Spatial Distribution of aerosol Black Carbon over India during Pre-monsoon Season. *Atmos. Environ.* 43: 1071–1078.

Dani, K.K., Ernest Raj, P., Devara, P.C.S., Pandithurai, G., Sonbawne, S.M., Maheskumar, R.S., Saha, S.K. and Jaya Rao, Y. (2012). Long-term Trends and Variability in Measured Multi-spectral Aerosol Optical Depth over

a Tropical Urban Station in India. *Int. J. Climatol.* 32: 153–160.

Dey, S., Tripathi, S.N., Singh, R.P. and Holben, B.N. (2004). Influence of Dust Storms on the Aerosol Optical Properties over the Indo-Gangetic Basin. *J. Geophys. Res.* 109: D20211.

Dey, S. and Tripathi, S.N. (2008). Aerosol Direct Radiative Effects over Kanpur in the Indo-Gangetic Basin, Northern India, 2008. Long-term (2001-2005) Observations and Implications to Regional Climate. *J. Geophys. Res.* 113: D04212.

Dubovik, O., Holben, B.N., Eck, T.F., Smirnov, A., Kaufman, Y.J., King, M.D., Tanrè, D. and Slutsker, I. (2002). Variability of Absorption and Optical Properties of Key Aerosol Types Observed in Worldwide Locations. *J. Atmos. Sci.* 59: 590–608.

Eck, T.F., Holben, B.N., Dubovic, O., Smirnov, A., Slutsker, I., Lobert, J.M. and Ramanathan, V. (2001). Column-integrated Aerosol Optical Properties over the Maldives during the Northeast Monsoon for 1998-2000. *J. Geophys. Res.* 106: 28555–28566.

Eck, T.F., Holben, B.N., Sinyuk, A., Pinker, R.T., Goloub, P., Chen, H., Chatenet, B., Li, Z., Singh, R.P., Tripathi, S.N., Reid, J.S., Giles, D.M., Dubovik, O., O'Neill, N.T., Smirnov, A., Wang, P. and Xia, X. (2010). Climatological Aspects of the Optical Properties of Fine/Coarse Mode Aerosol Mixtures. *J. Geophys. Res.* 115: D19205.

Ganguly, D., Jayaraman, A. and Gadhavi, H. (2006). Physical and Optical Properties of Aerosols over an Urban Location in Western India Seasonal Variabilities. *J. Geophys. Res.* 111: D24206,

Gautam, R., Hsu, N.C., Kafatos, M. and Tsay, S.C. (2007). Influences of Winter Haze on Fog/Low Cloud over the Indo-Gangetic Plains, *J. Geophys. Res.* 112: D05207.

Gautam, R., Hsu, N.C. and Lau, K.M. (2010). Premonsoon Aerosol Characterization and Radiative Effects over the Indo-Gangetic Plains: Implications for Regional Climate Warming. *J. Geophys. Res.* 115: D17208.

Gautam, R., Hsu, N.C., Tsay, S.C., Lau, K.M., Holben, B.N., Bell, S., Smirnov, A., Li, C., Hansell, R., Ji, Q., Payra, S., Aryal, D., Kayastha, R. and Kim, K.M. (2011). Accumulation of Aerosols over the Indo-Gangetic Plains and Southern Slopes of the Himalayas: Distribution, Properties and Radiative Effects during the 2009 Pre-monsoon Season. *Atmos. Chem. Phys.* 11: 12841–12863.

Giles, D.M., Holben, B.N., Tripathi, S.N., Eck, T.F., Newcomb, W., Slutsker, I., Dickerson, R., Thompson, A., Mattoo, S., Wang, S., Singh, R., Sinyuk, A. and Schafer, J. (2011). Aerosol Properties over the Indo-Gangetic Plain: A 1 Mesoscale Perspective from the TIGERZ Experiment. *J. Geophys. Res.* 116: D18203.

Gogoi, M., Pathak, B., Moorthy, K.K., Bhuyan, P.K., Suresh Babu, S., Bhuyan, K. and Kalita, G. (2011). Mutli-year Investigations of near Surface and Columnar Aerosols over Dibrugarh, North-Eastern Location of India: Heterogeneity in Source Impacts. *Atmos. Environ.* 45: 1714–1724.

Goloub, P., Deuze, J.L., Herman, M., Tanre, D., Chiapello, I., Roger, B. and Singh, R.P. (2001). Aerosol Remote Sensing over Land from the Spaceborne Polarimeter

POLDER, IRS 2000: Current Problems in Atmospheric Radiation, p. 113–116.

Guleria, R.P., Kuniyal, J.C., Rawat, P.S., Thakur, H.K., Sharma, M., Sharma, N.L., *et al.* (2011). Aerosols Optical Properties in Dynamic Atmosphere in the Northwestern Part of the Indian Himalaya: A Comparative Study from Ground and Satellite Based Observations. *Atmos. Res.* 101: 726–738.

Holben, B.N., Tanre, D., Smirnov, A., Eck, T.F., Slutsker, I., Abuhassan, N., *et al.* (2001). An Emerging Ground-based Aerosol Climatology: Aerosol Optical Depth from AERONET. *J. Geophys. Res.* 106: 67–97.

Kaskaoutis, D.G., Kambezidis, H.D., Hatzianastassiou, N., Kosmopoulos, P. and Badarinath K.V.S. (2007a). Aerosol Climatology: On the Discrimination of the Aerosol Types over Four AERONET Sites. *Atmos. Chem. Phys. Discuss.* 7: 6357–6411.

Kaskaoutis, D.G., Kambezidis, H.D., Hatzianastassiou, N., Kosmopoulos, P.G. and Badarinath, K.V.S. (2007b). Aerosol Climatology: Dependence of the Ångström Exponent on Wavelength over Four AERONET Sites. *Atmos. Chem. Phys. Discuss.* 7: 7347–7397.

Kaskaoutis, D.G. and Kambezidis, H.D. (2008). Comparison of the Ångström Parameters Retrieval in Different Spectral Ranges with The use of Different Techniques. *Meteorol. Atmos. Phys.* 99: 233–246.

Kaskaoutis, D.G., Badarinath, K.V.S., Kharol, S.K., Sharma, A.R. and Kambezidis, H.D. (2009). Variations in the Aerosol Optical Properties and Types over the Tropical Urban Site of Hyderabad, India. *J. Geophys. Res* 114: D22204.

Kaskaoutis, D.G., Kalapureddy, M.C.R. Moorthy, K.K., Devara, P.C.S., Nastos, P.T., Kosmopoulos, P.G. and Kambezidis, H.D. (2010). Heterogeneity in Pre-monsoon Aerosol Types over the Arabian Sea Deduced from Shipboard Measurements of Spectral AODs. *Atmos. Chem. Phys.* 10: 4893–4908.

Kaskaoutis, D.G., Kharol, S.K., Sinha, P.R., Singh, R.P., Badarinath, K.V.S., Mehdi, W. and Sharma, M. (2011a). Contrasting Aerosol Trends over South Asia during the Last Decade Based on MODIS Observations. *Atmos. Meas. Tech. Discuss.* 4: 5275–5323.

Kaskaoutis, D.G., Kharol, S.K., Sinha, P.R., Singh, R.P., Kambezidis, H.D., Sharma, A.R. and Badarinath, K.V.S. (2011). Extremely Large Anthropogenic-aerosol Contribution to Total Aerosol Load over the Bay of Bengal during Winter Season. *Atmos. Chem. Phys.* 11: 7097–7117.

Kaskaoutis, D.G., Singh, R.P., Gautam, R., Sharma, M., Kosmopoulos, P.G. and Tripathi, S.N. (2012). Variability and Trends of Aerosol Properties over Kanpur, Northern India Using AERONET Data (2001-10). *Environ. Res. Lett.* 7: 024003.

Kharol, S.K., Badarinath. K.V.S., Sharma, A.R., Mahalakshmi, D.V., Singh, D. and Krishna, P.V. (2012) Black Carbon Aerosol Variations over Patiala City, Punjab, India - A Study during Agriculture Crop Residue Burning Period Using Ground Measurements and Satellite Data. *J. Atmos. Sol. Terr. Phys.* 84–85: 45–51.

Lau, K.M., Kim, M.K. and Kim, K.M. (2006). Asian Summer Monsoon Anomalies Induced by Aerosol Direct Forcing: The Role of the Tibetan Plateau. *Clim. Dyn.* 26: 855–864.

Lawrence, M.G. and Lelieveld, J. (2010). Atmospheric Pollutant Outflow from Southern Asia: A Review. *Atmos. Chem. Phys.* 10: 11017–11096.

Lee, J., Kim, J., Song, C.H., Kim, S.B., Chun, Y.S., Sohn, B.J. and Holben, B.N. (2010). Characteristics of Aerosol Types from AERONET Sun Photometer Measurements. *Atmos. Environ.* 44: 3110–3117.

Lodhi, N.K., Beegum, S.N., Singh, S. and Kumar, K. (2013). Aerosol Climatology at Delhi in the Western Indo-Gangetic Plain: Microphysics, Long-term Trends, and Source Strengths. *J. Geophys. Res.* 118, doi: 10.1002/jgrd.50165.

Lu, Z., Zhang, Q. and Streets, D.G. (2011). Sulfur Dioxide and Primary Carbonaceous Aerosol Emissions in China and India, 1996–2010. *Atmos. Chem. Phys.* 11: 9839–9864.

Mishra, A.K. and Shibata, T. (2012). Synergistic Analyses of Optical and Microphysical Properties of Agricultural Crop Residue Burning Aerosols over the Indo-Gangetic Basin (IGB). *Atmos. Environ.* 57: 205–218.

Mishra, A.K., Srivastava, A. and Jain, V.K. (2013). Spectral Dependency of Aerosol Optical Depth and Derived Aerosol Size Distribution over Delhi: An Implication to Pollution Source. *Sustainable Environ. Res.* 23: 113–128.

Moorthy, K.K., Suresh Babu, S., Manoj, M.R. and Satheesh, S.K. (2013). Buildup of Aerosols over the Indian Region. *Geophys. Res. Lett.* 40: 1011–1014, doi: 10.1002/grl.50165.

Morys, M., Mims III, F.M., Hagerup, S., Anderson, S.E., Baker, A., Kia, J. and T. Walkup (2001). Design, Calibration, and Performance of MICROTOPS II Handheld Ozone Monitor and Sun Photometer. *J. Geophys. Res.* 14:573– 582.

Pathak, B., Bhuyan, P.K. and Gogoi, M. (2012). Seasonal Heterogeneity in Aerosol Types over Dibrugarh-North-Eastern India. *Atmos. Environ.* 47: 307–315.

Prasad, A.K., Singh, R.P. and Kafatos, M. (2006). Influence of Coal Based Thermal Power Plants on Aerosol Optical Properties in the Indo-Gangetic Basin. *Geophys. Res. Lett.* 33: L05805.

Prasad, A.K. and Singh, R.P. (2007). Changes in Aerosol Parameters during Major Dust Storm Events (2001–2005) over the Indo-Gangetic Plains Using AERONET and MODIS Data. *J. Geophys. Res.* 112: D09208.

Prasad, A.K., Singh, S., Chauhan, S.S., Srivastava, M.K., Singh, R.P. and Singh, R. (2007). Aerosol Radiative Forcing over the Indo-Gangetic Plains during Major Dust Storms. *Atmos. Environ.* 41: 6289–6301.

Prasad, A.K., Singh, R.P. and Kafatos, M. (2012). Influence of Coal-based Thermal Power Plants on the Spatial-temporal Variability of Tropospheric NO_2 Column over India. *Environ. Monit. Assess.* 184: 1891–1907 doi: 10.1007/s10661-011-2087-6.

Rajeevan, M., Bhate, J., Kale, J.D. and Lal, B. (2006). High Resolution Daily Gridded Rainfall Data for the Indian Region: Analysis of Break and Active Monsoon Spells. *Curr. Sci.* 91: 296–306.

Ramanathan, V., Chung, C., Kim, D., Bettge, T., Buja, L.,

Kiehl, J.T., Washington, W.M., Fu, Q., Sikka, D.R. and Wild, M. (2005). Atmospheric Brown Clouds: Impacts on South Asian Climate and Hydrological Cycle. *PNAS* 102: 5326–5333.

Ramachandran, S. and Cherian, R. (2008). Regional and Seasonal Variations in Aerosol Optical Characteristics and Their Frequency Distributions over India during 2001–2005. *J. Geophys. Res.* 113: D08207.

Ramachandran, S., Kedia, S. and Srivastava, R. (2012a). Aerosol Optical Depth Trends over Different Regions of India. *Atmos. Environ.* 49: 338–347.

Ramachandran, S., Srivastava, R., Kedia, S. and Rajesh, T.A. (2012b). Contribution of Natural and Anthropogenic Aerosols to Optical Properties and Radiative Effects over an Urban Location. *Environ. Res. Lett.* 7: 034028.

Rao, V.B., Arai, E., Franchito, S.H., Shimabukuro, Y.E., Ramakrishna, S.S.V.S. and Naidu, C.V. (2011). The Thar, Rajputana Desert Unprecedented Rainfall in 2006 and 2010: Effect of Climate Change? *Geofis. Int.* 4: 363–370.

Schuster, G.L., Dubovik, O. and Holben, B.N. (2006). Ångström Exponent and Bimodal Aerosol Size Distributions. *J. Geophys. Res.* 111: D07207.

Sharma, A.R., Kharol, S.K., Badarinath, K.V.S. and Singh, D. (2010). Impact of Agriculture Crop Residue Burning on Atmospheric Aerosol Loading – A Study over Punjab State, India. *Ann. Geophys.* 28: 367–379.

Sharma, D., Singh, D. and Kaskaoutis, D.G. (2012). Impact of Two Intense Dust Storms on Aerosol Characteristics and Radiative Forcing over Patiala, in the North-West India. *Adv. Meteorol.* 2012: 956814, doi: 10.1155/2012/956814.

Singh, R.P., Dey, S., Tripathi, S.N., Tare, V. and Holben, B.N. (2004). Variability of Aerosol Parameters over Kanpur, Northern India. *J. Geophys. Res.* 109: D23206.

Singh, R.P. (2010). Interactive Comment on "Inferring Absorbing Organic Carbon Content from AERONET Data" by A. Arola *et al.*, *Atmos. Chem. Phys. Discuss.* 10: C7718–C7718.

Singh, R.P. and Sharma, M. (2012). Enhancement of BC Concentration Associated with Diwali Festival in India, 2012 IEEE International Geoscience and Remote Sensing Symposium (IGARSS) Book Series: IEEE International Symposium on Geoscience and Remote Sensing IGARSS, p. 3685–3688.

Singh, S., Nath, S., Kohli, R. and R. Singh. (2005). Aerosols over Delhi during Pre-monsoon Months: Characteristics and Effects on Surface Radiation Forcing. *Geophys. Res. Lett.* 32: L13808

Singh, S., Soni, K., Bano, T., Tanwar, R.S., Nath, S. and Arya, B.C. (2010). Clear-sky Direct Aerosol Radiative Forcing Variations over Mega-city Delhi. *Ann. Geophys.* 28: 1157–1166.

Sinha, P.R., Kaskaoutis, D.G., Manchanda, R.K. and Sreenivasan, S. (2012). Characteristics of Aerosols over Hyderabad, in Southern Peninsular India with the use of different techniques. *Ann. Geophys.* 30: 1393–1410.

Sinha, P.R., Dumka, U.C., Manchanda, R.K., Kaskaoutis, D.G., Sreenivasan, S., Moorthy, K.K. and Suresh, B.S. (2013). Contrasting Aerosol Characteristics and Radiative

Forcing over Hyderabad, India Due to Seasonal Meso-scale and Synoptic Scale Processes. *Q. J. R. Meteorolog. Soc.* 139: 434–450.

Soni, K., Singh, S., Tanwar, R.S. and Nath, S. (2011), Wavelength Dependence of the Aerosol Angstrom Exponent and Its Implications over Delhi, India. *Aerosol Sci. Technol.* 45:1488–1498.

Srivastava, A.K., Tripathi, S.N., Dey, S., Kanawade, V.P. and Tiwari, S. (2012a). Inferring Aerosol Types over the Indo-Gangetic Basin from Ground Based Sun Photometer Measurements. *Atmos. Res.* 109: 64–75.

Srivastava, A.K., Singh, S., Tiwari, S. and Bisht, D.S. (2012b). Contribution of Anthropogenic Aerosols in Direct Radiative Forcing and Atmospheric Heating Rate over Delhi in the Indo-Gangetic Basin. *Environ. Sci. Pollut. Res. Int.* 19: 1144–1158.

Srivastava, A.K., Tiwari, S., Devara, P.C.S., Bisht, D.S., Srivastava, M.K., Tripathi, S.N., Goloub, P. and Holben, B.N. (2012c). Pre-monsoon Aerosol Characteristics over the Indo-Gangetic Basin: implications to Climatic Impact. *Ann. Geophys.* 29: 789–804.

Srivastava, R. and Ramachandran, S. (2013). The Mixing State of aerosols over the Indo-Gangetic Plain and Its Impact on Radiative Forcing. *Q. J. R. Meteorolog. Soc.* 139: 137–151.

Tiwari, S. and Singh, A.K. (2013). Variability of Aerosol Parameters Derived from Ground and Satellite Measurements over Varanasi Located in Indo-Gangetic Basin. *Aerosol Air Qual. Res.* 13: 627–638.

Vijayakumar, K. and Devara, P.C.S. (2013). Study of Aerosol Optical Depth, Ozone, and Precipitable Water Vapour Content over Sinhagad, a High-altitude Station in the Western Ghats. *Int. J. Remote Sens.* 34: 613–630.

Vinoj, V., Satheesh, S.K., Suresh, B.S. and Moorthy, K.K. (2004). Large Aerosol Optical Depths Observed at an Urban Location in Southern India associated with Rain-Deficit Summer Monsoon Season. *Ann. Geophys.* 22: 3073–3077.

Wang, S., Fang, L., Gu, X., Yua, T. and Gao, J. (2011). Comparison of Aerosol Optical Properties from Beijing and Kanpur. *Atmos. Environ.* 45: 7406–7414.